Title	Characteristics of a hydraulic jump in Bingham fluid(Main article)
Author(s)	Shu, Jian Jun; Zhou, Jian Guo
Citation	Shu, J. J., & Zhou, J. G. (2006). Characteristics of a hydraulic jump in Bingham fluid. Journal of hydraulic research, 44(3), 421-426.
Date	2006
URL	http://hdl.handle.net/10220/7142
Rights	© 2006 International Association of Hydraulic Engineering and Research. This is the author created version of a work that has been peer reviewed and accepted for publication by Journal of hydraulic research, International Association of Hydraulic Engineering and Research. It incorporates referee's comments but changes resulting from the publishing process, such as copyediting, structural formatting, may not be reflected in this document. The published version is available at: [DOI: http://dx.doi.org/10.1080/00221686.2006.9521693]

Characteristics of a hydraulic jump in Bingham fluid

Jian-Jun SHU[a*] and Jian Guo ZHOU[b]

[a] School of Mechanical & Aerospace Engineering,

Nanyang Technological University, 50 Nanyang Avenue, Singapore 639798

[b] Civil Engineering Division, Manchester School of Engineering,

University of Manchester, Manchester M13 9PL, England, United Kingdom

Abstract

Hydraulic jump taking place in Bingham fluid over a horizontal plate has been studied. The formulas for conjugate depths, bottom shear stress and critical depth are established. Since no exact analytical solution in closed form can be obtained for conjugate depths, an approximate formula is developed. This formula can provide good results with an error less than 4%. The analytical results reveal that the critical depth and the ratio of conjugate depths increase until the bottom shear stress exceeds a certain value and then decrease afterwards. The bottom shear stress downstream of hydraulic jump is smaller than that upstream. The results are verified by experimental data and observations available in the literature.

Keywords: Bingham fluid; hydraulic jump; non-Newtonian fluid

*Author to whom correspondence should be addressed.

1 Introduction

Muddy debris flow (Coussot 1994a,b), a mixture of water and cohesive clay particles, behaves like an inelastic non-Newtonian fluid and is often encountered in industry and nature, *e.g.* sewage sludge, submarine landslides, mountain mudflows, coal slurries, drilling mud. Bingham fluid is widely used as an ideal and simple model in the study of non-Newtonian fluid. In this model, the process of cross-link formation and destruction is instantaneous. The thixotropic tendency has been ignored and the excess deviatoric stress τ over the yield stress τ_0 is assumed to be a linear function of the strain rate $\partial U/\partial y$ (Bingham 1922),

$$\mu_0 \frac{\partial U}{\partial y} = \begin{cases} 0 & \text{if } |\tau| < \tau_0 \\ (\tau - \tau_0)\ \mathrm{sgn}(\frac{\partial U}{\partial y}) & \text{if } |\tau| \geq \tau_0 \end{cases} \tag{1}$$

where μ_0 is the fluid viscosity.

An experimental study conducted by Ogihara & Miyazawa (1994) showed that the characteristics of hydraulic jump in Bingham fluid were not able to be fully described by the classical (Newtonian) hydraulic jump formulation. Hydraulic jump in non-Newtonian fluid was theoretically studied by Ng & Mei (1994) and Liu & Mei (1994), who provided an analysis of jump condition. Unfortunately, the analysis of conjugate depths and bottom shear stress, which are often of most interest in practical engineering, has not fully been exploited. In this paper, an adequate model for hydraulic jump in Bingham fluid has been developed. Hence, the formulas for conjugate depths, bottom shear stress and critical depth are derived. The results are compared with available experimental data.

2 Hydraulic jump

From the engineering viewpoint, the conjugate depths, bottom shear stress and critical depth are of primary importance in hydraulic jump. The basic equations for these characteristic quantities can be established based on the integral continuity and momentum equations, combined with the properties of Bingham fluid.

Applying the integral continuity equation, we have

$$q = \int_0^{h_1} U_1(y)dy = \int_0^{h_2} U_2(y)dy \tag{2}$$

where q is the discharge per unit width and subscripts 1 and 2 denote the upstream and downstream of hydraulic jump respectively for all quantities (see Fig. 1 and Fig. 2).

The upstream and downstream flows of hydraulic jump taking place in Bingham fluid over a horizontal plate can be treated as two-dimensional, fully-developed, half-Poiseuille flows. $U(y)$ in Eq. (2) can be expressed as (Liu & Mei 1989)

$$U(\xi) = \begin{cases} U_0 & 1-\lambda \le \xi \le 1 \\ U_0\left[1-\left(\frac{1-\lambda-\xi}{1-\lambda}\right)^2\right] & 0 \le \xi < 1-\lambda \end{cases} \tag{3}$$

where $\xi = y/h$, $\lambda = \tau_0/\tau_w$; τ_w is the shear stress at the bottom; $p = \rho g(h-y)$ is the hydrostatic pressure and other symbols are shown in Fig. 1. Substitution of Eq. (3) into Eq. (2) leads to

$$\frac{1}{3}U_{01}h_1(2+\lambda_1) = \frac{1}{3}U_{02}h_2(2+\lambda_2). \tag{4}$$

Similarly, according to the integral momentum equation, we obtain

$$\int_0^{h_1} \rho(\vec{V}_1 \cdot \vec{n}_1)U_1 dy + \int_0^{h_2} \rho(\vec{V}_2 \cdot \vec{n}_2)U_2 dy = \int_0^{h_1} p_1 dy - \int_0^{h_2} p_2 dy. \tag{5}$$

Integrating Eq. (5) with Eq. (3) results in

$$\frac{8+7\lambda_2}{15}U_{02}^2 h_2 - \frac{8+7\lambda_1}{15}U_{01}^2 h_1 = \frac{g}{2}(h_1^2 - h_2^2). \tag{6}$$

Generally, the flow conditions upstream of hydraulic jump are known, *i.e.* U_{01}, h_1 and λ_1. There are two equations, Eqs (4) and (6), which obviously are not sufficient to determine the three unknowns U_{02}, h_2 and λ_2. An additional equation must be provided. This comes from the shear stress in Bingham fluid.

If Eq. (1) is applied to the upstream of hydraulic jump, we have

$$\mu_0 \frac{\partial U_1}{\partial y}\bigg|_{y=0} = (\tau_1 - \tau_0)|_{y=0}. \tag{7}$$

Substitution of Eq. (3) into the above equation results in

$$\frac{2\mu_0 U_{01}}{h_1(1-\lambda_1)} = (\tau_{w1} - \tau_0). \tag{8}$$

Similarly, we have

$$\frac{2\mu_0 U_{02}}{h_2(1-\lambda_2)} = (\tau_{w2} - \tau_0). \tag{9}$$

Combining Eqs (8) and (9) gives

$$\frac{U_{01}h_2}{U_{02}h_1} = \frac{\lambda_2}{\lambda_1}\left(\frac{1-\lambda_1}{1-\lambda_2}\right)^2. \tag{10}$$

Eqs (4), (6) and (10) are the basic equations for the three unknowns $U_{02},\ h_2$ and λ_2 for hydraulic jump in Bingham fluid.

It should be noted that there are only two unknowns, $U_{02},\ h_2$, for hydraulic jump in Newtonian fluid, whereas there are three, $U_{02},\ h_2$ and λ_2, for hydraulic jump in Bingham or non-Newtonian fluid.

A further mathematical consideration indicates that there are no analytical solutions to the basic equations, but an asymptotic solution can be developed.

Substitution of Eq. (4) into Eqs (6) and (10) respectively gives

$$\frac{8+7\lambda_2}{\eta}\left(\frac{2+\lambda_1}{2+\lambda_2}\right)^2-(8+7\lambda_1)=\frac{5(2+\lambda_1)^2}{6F_{r1}^2}(1-\eta^2) \tag{11}$$

$$\eta^2\frac{2+\lambda_2}{2+\lambda_1}=\frac{\lambda_2}{\lambda_1}\left(\frac{1-\lambda_1}{1-\lambda_2}\right)^2 \tag{12}$$

where $\eta=h_2/h_1$ and $F_{r1}=V_{01}/\sqrt{gh_1}$ is the Froude number, in which V_{01} is the depth-averaged velocity defined by

$$V_0=\frac{1}{h}\int_0^h U(y)dy=\frac{1}{3}U_0(2+\lambda). \tag{13}$$

In the present context, the hydraulic jump is a discontinuous transition from the supercritical (upstream) flow ($F_{r1}>1$) to the subcritical (downstream) flow ($F_{r2}<1$).

Combining Eq. (11) with Eq. (12) leads to a fifth-order polynomial in term of either η or λ_2. According to the algebraic field theory, there are no analytic solutions for any fifth-order polynomial. Numerical solutions will be given in Section 4.

The form of Eq. (11) suggests that an asymptotic solution can be derived in the case of $\eta\to 1$ as follows:

Defining

$$f(\lambda_2)=\frac{8+7\lambda_2}{(2+\lambda_2)^2}, \tag{14}$$

Eq. (11) becomes

$$\frac{f(\lambda_2)}{\eta}(2+\lambda_1)^2-(8+7\lambda_1)=\frac{5(2+\lambda_1)^2}{6F_{r1}^2}(1-\eta^2). \tag{15}$$

With reference to Eq. (12), λ_2 is a function of η. Thus $f(\lambda_2)$ can be expanded in terms of $(\eta-1)$ by using the Taylor series

$$f(\lambda_2)=f(\lambda_2)|_{\eta\to1}+\left.\frac{df(\lambda_2)}{d\eta}\right|_{\eta\to1}(\eta-1)+O(\eta-1)^2. \tag{16}$$

Obviously $\lambda_2 \to \lambda_1$ as $\eta \to 1$, hence

$$f(\lambda_2)|_{\eta\to 1} = f(\lambda_1). \tag{17}$$

According to the chain rule,

$$\frac{df(\lambda_2)}{d\eta} = \frac{df(\lambda_2)}{d\lambda_2}\frac{d\lambda_2}{d\eta}, \tag{18}$$

we have

$$\left.\frac{df(\lambda_2)}{d\eta}\right|_{\eta\to 1} = -\frac{(2+7\lambda_1)(1-\lambda_1)\lambda_1}{(2+\lambda_1)^2(1+\lambda_1+\lambda_1^2)}. \tag{19}$$

Substitution of Eqs (17) and (19) into Eq. (16) yields

$$f(\lambda_2) = \frac{8+7\lambda_1}{(2+\lambda_1)^2} - \frac{(2+7\lambda_1)(1-\lambda_1)\lambda_1}{(2+\lambda_1)^2(1+\lambda_1+\lambda_1^2)}(\eta-1) + O(\eta-1)^2. \tag{20}$$

By substituting Eq. (20) into Eq. (15) and rearrangement, we obtain

$$\eta(1+\eta) = \frac{6}{5}F_{r1}^2\frac{8+17\lambda_1+20\lambda_1^2}{(1+\lambda_1+\lambda_1^2)(2+\lambda_1)^2}\left[1+O(\eta-1)\right]. \tag{21}$$

By ignoring terms of order $(\eta-1)$ and higher, Eq. (21) becomes

$$\eta^2 + \eta - 2C_0F_{r1}^2 = 0 \tag{22}$$

with

$$C_0 = \frac{3}{5}\frac{8+17\lambda_1+20\lambda_1^2}{(1+\lambda_1+\lambda_1^2)(2+\lambda_1)^2}. \tag{23}$$

The analytical solution to Eq. (22) is

$$\eta = \frac{1}{2}\left[\sqrt{1+8C_0F_{r1}^2}-1\right]. \tag{24}$$

The energy dissipation due to hydraulic jump is referred to as the head loss ΔH. Solving the Bernoulli (energy) equation along points on the fluid surface

$$\frac{U_{01}}{2g} + h_1 = \frac{U_{02}}{2g} + h_2 + \Delta H \tag{25}$$

and eliminating U_{01} and U_{02} yield:

$$\Delta H = (h_2-h_1)\left[\frac{(h_2-h_1)^2}{4C_1h_2h_1} + \frac{1-C_1}{C_1}\right]\left[1+O(h_2-h_1)\right] \tag{26}$$

where

$$C_1 = \frac{8+7\lambda_1}{15}. \tag{27}$$

Eq. (24) is the approximate formula for the conjugate depths. Theoretically, only under the condition that η is close to unity, can it be valid. However, the analysis and

discussion in 4.3 will indicate that it can be used with a good accuracy in situations where η is larger than unity. After η is obtained through Eq. (24), U_{02} and λ_2 can be calculated by Eqs (4) and (12), respectively.

It is found that C_0 reaches the maximum, *i.e.* $C_{0max} = 1.22$ when $\lambda_1 = 0.213$ or $\tau_0/\tau_{w1} = 0.213$. Since Bingham fluid consists of two distinct regions, plug and shear regions (Fig. 1), the existence of such maximum suggests that hydraulic jump is hereby coupled between the effects of the two regions. When $0 \leq \lambda_1 \leq 0.213$, the shear region dominates hydraulic jump and the relative jump height h_2/h_1 is an increasing function of λ_1; when $0.213 \leq \lambda_1 \leq 1$, the plug region dominates hydraulic jump and h_2/h_1 is a decreasing function of λ_1.

Two points are worthy mentioning. Firstly, analytical solution (24) for hydraulic jump in Bingham fluid can be extended to two extreme cases — the solution for hydraulic jump in a fully-developed Newtonian viscous flow when $\lambda_1 = 0$ or $C_0 = 6/5$ and that in an inviscid flow when $\lambda_1 = 1$ or $C_0 = 1$. Secondly, the bottom shear stress τ_{w2} downstream is always smaller than τ_{w1} upstream of hydraulic jump in Bingham fluid, which becomes very clear from Eq. (12).

3 Critical depth

When the conjugate depths upstream and downstream of hydraulic jump are the same, such flow is referred to as a critical flow. Since approximate formula (24) becomes an exact solution when $\eta = 1$, the formula for critical depth is then obtained as

$$h_c = \sqrt[3]{C_0 \frac{q^2}{g}} \tag{28}$$

by setting $\eta = 1$ and $h_2 = h_1 = h_c$ with $F_{r1} = q/\sqrt{gh_c^3}$ in (24). For a critical flow, $\lambda_1 = \lambda_2 = \lambda$ in Eq. (23).

Eq. (28) is the formula for the critical depth in Bingham fluid. Clearly, it is the solution for a fully viscous flow if $\lambda = 0$ or $C_0 = 6/5$ and that for a fully inviscid flow if $\lambda = 1$ or $C_0 = 1$. h_c changes with λ in the interval $0 < \lambda < 1$. The feature of the function C_0 shows that h_c increases with λ for $0 \leq \lambda_1 \leq 0.213$ and decreases for $0.213 < \lambda \leq 1$. h_c reaches the maximum value of $1.068\sqrt[3]{q^2/g}$ at $\lambda = 0.213$, where the critical flow is coupled between the effects of plug and shear regions. The shear region dominates the critical flow in the interval $0 \leq \lambda_1 \leq 0.213$ and the plug region dominates the flow in the interval

$0.213 < \lambda \leq 1$. The features are also shown in Fig. 3 in terms of h_c/h_q versus τ_0/τ_w or λ, where $h_q = \sqrt[3]{q^2/g}$. Obviously, the critical depth is always greater than that in a fully inviscid flow, and it is also higher than that in a fully viscous flow for $0 \leq \lambda \leq 0.41$, but lower for $0.41 < \lambda \leq 1$.

4 Numerical solutions of jump equations

As pointed out in Section 2, Eqs (11) and (12) cannot be solved analytically. Hence a numerical method is used to solve them. In the present study, Newton's method is applied to obtain the numerical solutions.

4.1 Conjugate depths

The numerical results for the conjugate depths are plotted in Figs 4 and 5. It is clearly seen that η or h_2/h_1 is almost a linear function of F_{r1} but is not a linear function of τ_0/τ_{w1} or λ_1. η always increases with F_{r1} but it may increase or decrease depending on the value of λ_1, which can be seen from the figures. As expected, there is one peak or maximum value of η as λ_1 changes from 0 to 1.

4.2 Bottom shear stress

Since $\lambda = \tau_0/\tau_w$, λ represents the bottom shear stress τ_w. The numerical result of λ_2 versus λ_1 is shown in Fig. 6. As expected, λ_2 is always greater than λ_1 and is an increasing function of λ_1. The difference between the bottom shear stresses upstream and downstream of hydraulic jump increases with F_{r1} and vanishes at $\lambda_1 = 0$ or 1 in which $\lambda_2 = 0$ or 1, *i.e.* $\tau_{w2} = \tau_{w1}$.

4.3 Comparison of exact and approximate results

In Section 2, an approximate formula for conjugate depths is derived for η close to unity. In order to examine the accuracy, a comparison between the numerical results of Eqs (11) and (12) and the approximate ones of Eq. (24) is carried out. The relative errors defined by $(\eta|_{app} - \eta|_{num})/\eta|_{num}$, where $\eta|_{num}$ is calculated from Eqs (11) and (12) by numerical

method and $\eta|_{app}$ from Eq. (24), are plotted in Fig. 7. It clearly shows that the relative errors notably increase with F_{r1} for $F_{r1} < 10$. For most values of τ_0/τ_{w1}, the approximate results are greater than the numerical ones. In addition, the relative error increases with λ_1 until it is over a certain value which is a function of F_{r1}, and then decrease to zero. The computation has shown that the relative error is smaller than 4% in the range of $F_{r1} \leq 25$. Therefore, Eq. (24) is a reasonable approximate formula for conjugate depths. If $|\lambda_1 - 0.5| > 0.1$, even in the situation where η is much greater than unity, accuracy can still be retained.

5 Verification of the formulas

An experimental investigation of hydraulic jump in Bingham fluid was conducted by Ogihara & Miyazawa (1994), who studied the flow in a rectangular open channel by using the mixtures of water and bentonite, which were regarded as Bingham fluid and observed that the characteristics of hydraulic jump in the Bingham fluid were not able to be fully described by the classical (Newtonian) hydraulic jump formulation. Their experimental results are adopted to verify the theoretical results in the present study.

A comparison between the theoretical results and the experimental data for conjugate depths is plotted in Fig. 8. It can be seen that the experimental data are scattered. This may be due to the difficulty to measure the conjugate depths in hydraulic jump. The agreement between them is reasonably good.

For critical depths, the results between the theoretical ones and the experimental data are also compared and plotted in Fig. 9. The figure has clearly shown that there is a good agreement between them.

In addition, the critical depth increased dramatically was reported by Ogihara & Miyazawa (1994), when the dimensionless yield stress λ exceeded 0.1 in the experiment. This supports the theoretical result from the present study because h_c increases with λ in the range of $0 \leq \lambda \leq 0.213$. As indicated in Section 3, the critical depth continues to increase up to $\lambda = 0.213$. After that, it decreases with λ. Unfortunately, in the experiments, there is no further result available for this comparison.

6 Conclusions

The formulas for conjugate depths, bottom shear stress and critical depth have been derived. The critical depth reaches the maximum at $\lambda = 0.213$ where the critical flow is coupled between the effects of plug and shear regions. The bottom shear stress τ_{w2} is always smaller than τ_{w1}. Also, the approximate formula for conjugate depths with good accuracy is developed. The results are consistent with fully viscous or fully inviscid flows when $\lambda = 0$ or 1 respectively. The verification of the formulas is carried out by a comparison between the theoretical results and the experimental data. It has shown that the agreement is reasonably good. The formula also indicates that there is an apparent increase of critical depth for $\tau_0/\tau_w \leq 0.213$, which has been supported by the experimental observation that critical depth increased greatly for $\tau_0/\tau_w \geq 0.1$.

List of symbols

The following symbols are used in this paper:

C_0, C_1 = defined by (23) and (27) respectively ;

F_r = Froude number ;

g = acceleration due to gravity ;

h = conjugate depth ;

h_c = critical depth ;

h_q = critical depth in fully inviscid flow ;

p = pressure ;

q = discharge per width ;

$U, U_0, \vec{V},$ = velocity ;

V_0 = depth-averaged velocity ;

x, y = Cartesian coordinates;

ΔH = head loss;

η = ratio of conjugate depths;

λ = dimensionless yield stress;

μ_0 = viscosity coefficient;

ξ = dimensionless coordinate;

ρ = density;

τ = stress;

τ_0 = yield stress;

τ_w = bottom shear stress.

Subscripts

$1, 2$ = upstream, downstream.

References

[1] E.C. Bingham, *Fluidity and plasticity*, McGraw-Hill Book Company, Inc., New York, NY, USA (1922).

[2] P. Coussot, Steady, laminar, flow of concentrated mud suspensions in open-channel, *Journal of Hydraulic Research*, **32**(4) (1994a) 535-559.

[3] P. Coussot, Debris flow dynamics, *Houille Blanche-Revue Internationale de l Eau*, **49**(3) (1994b) 38-43 (in French).

[4] K.F. Liu and C.C. Mei, Slow spreading of a sheet of Bingham fluid on an inclined plane, *Journal of Fluid Mechanics*, **207** (1989) 505-529.

[5] K.F. Liu and C.C. Mei, Roll waves on a layer of a muddy fluid flowing down a gentle slope — a Bingham model, *Physics of Fluids*, **6** (1994) 2577-2590.

[6] C.O. Ng and C.C. Mei, Roll waves on a shallow layer of mud modelled as a power-law fluid, *Journal of Fluid Mechanics*, **263** (1994) 151-183.

[7] Y. Ogihara and N. Miyazawa, Hydraulic characteristics of flow over dam and hydraulic jump of Bingham fluid, *Journal of Hydraulic, Coastal and Environmental Engineering, Proceedings of the Japan Society of Civil Engineers*, **485**(II-26) (1994) 21-26 (in Japanese).

Figure Captions

Figure 1: Velocity profile for Bingham fluid over a horizontal plate

Figure 2: Sketch for a hydraulic jump

Figure 3: Critical depth versus dimensionless yield stress τ_0/τ_w

Figure 4: Conjugate depths versus Froude number F_{r1}

Figure 5: Conjugate depths versus dimensionless yield stress τ_0/τ_{w1}

Figure 6: τ_0/τ_{w2} versus τ_0/τ_{w1}

Figure 7: Relative error in percentage versus dimensionless yield stress τ_0/τ_{w1}

Figure 8: Comparison of the conjugate depth

Figure 9: Comparison of the critical depth

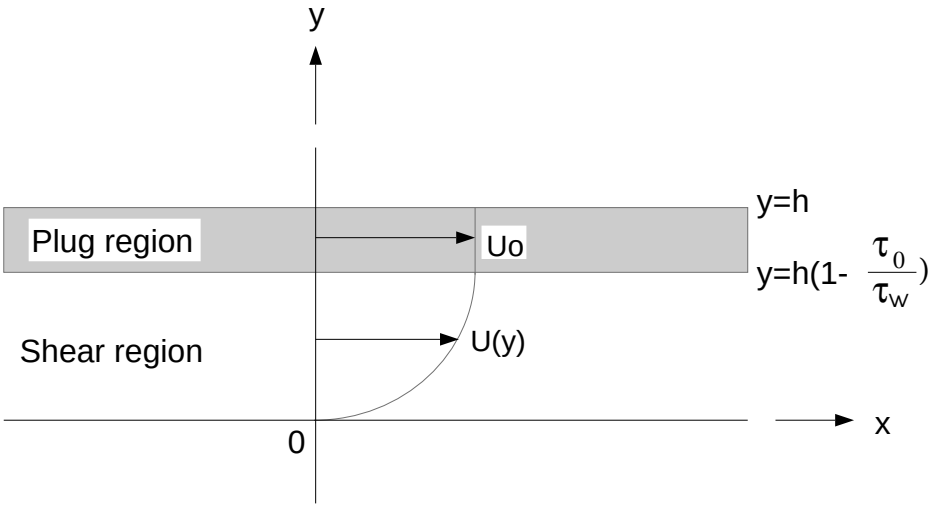

Figure 1: Velocity profile for Bingham fluid over a horizontal plate

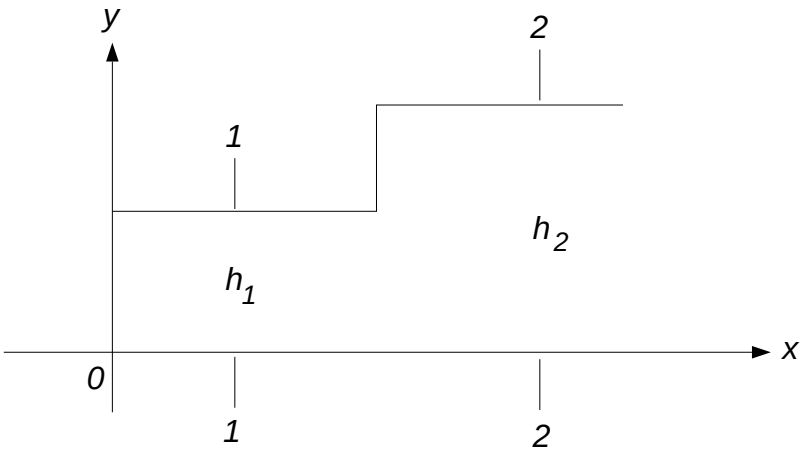

Figure 2: Sketch for a hydraulic jump

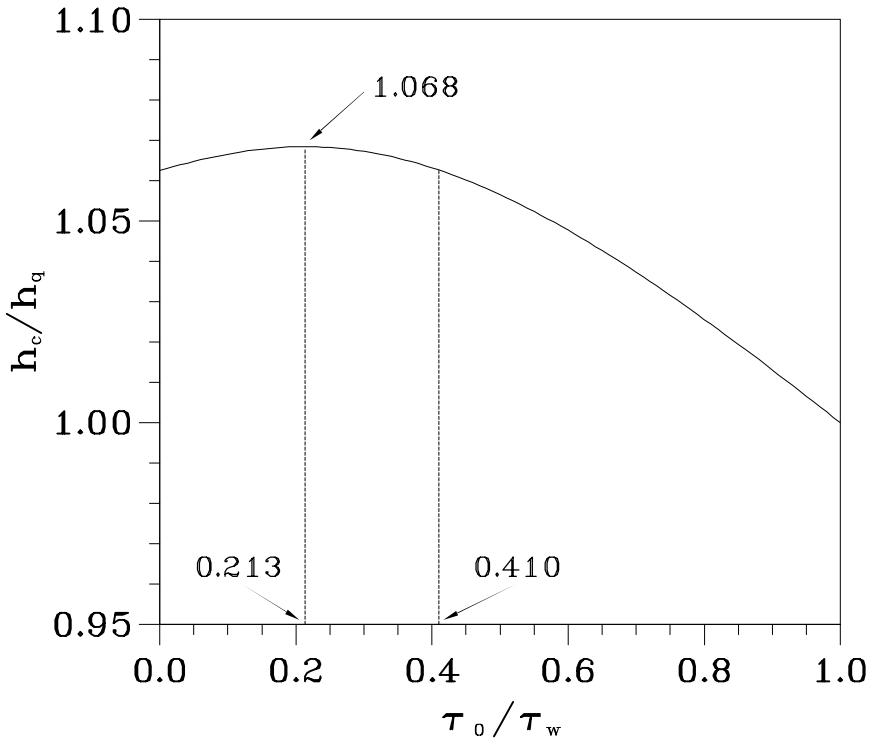

Figure 3: Critical depth versus dimensionless yield stress τ_0/τ_w

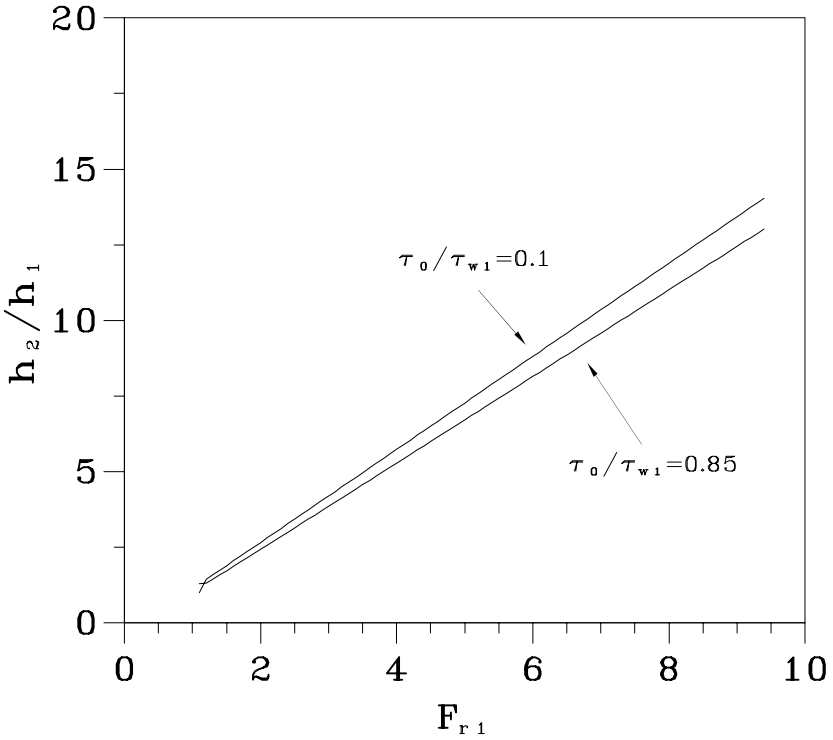

Figure 4: Conjugate depths versus Froude number F_{r1}

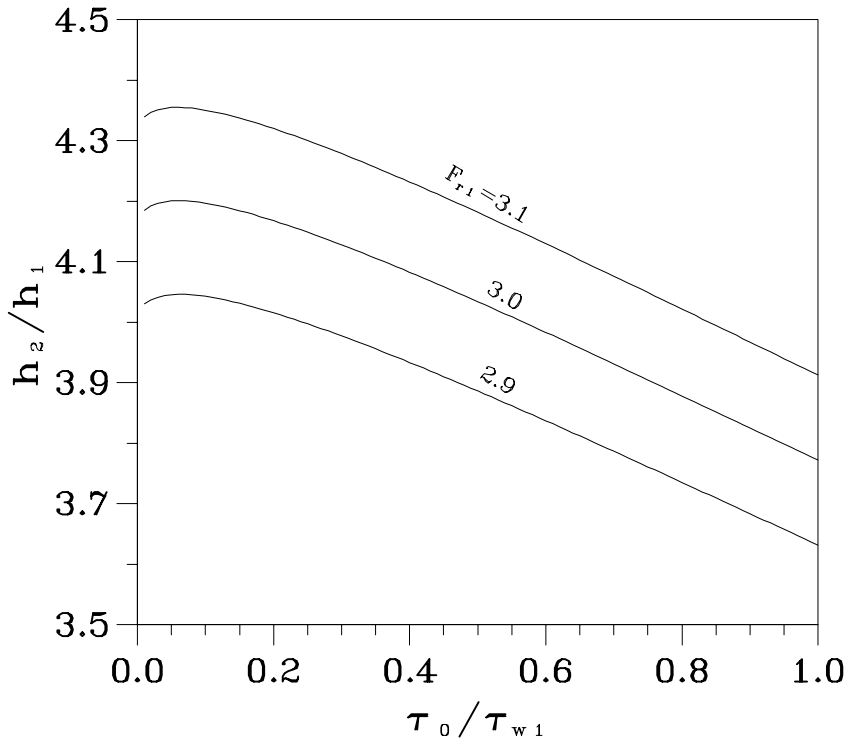

Figure 5: Conjugate depths versus dimensionless yield stress τ_0/τ_{w1}

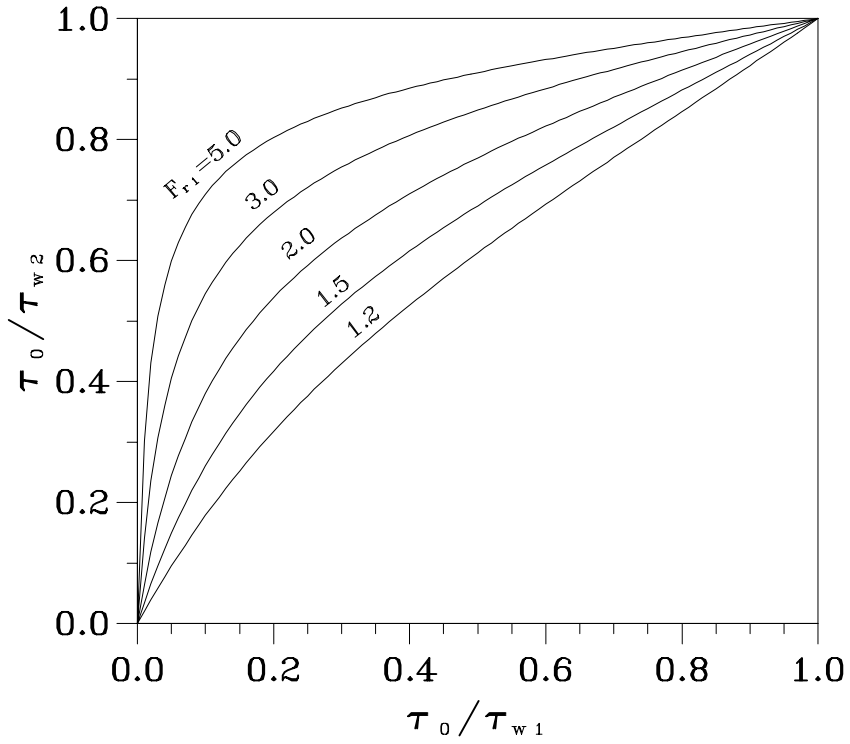

Figure 6: τ_0/τ_{w2} versus τ_0/τ_{w1}

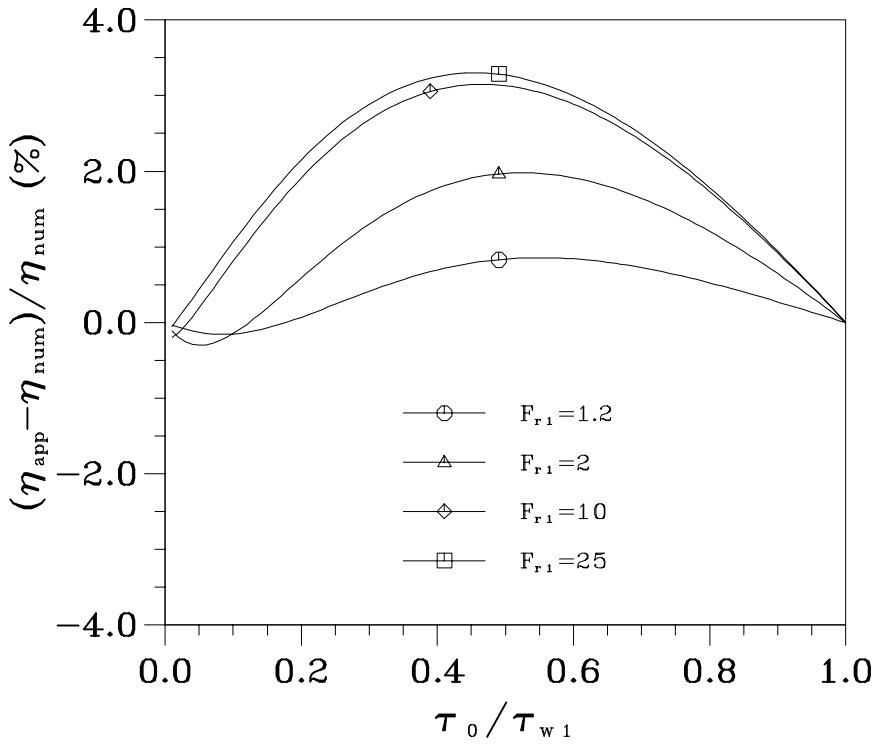

Figure 7: Relative error in percentage versus dimensionless yield stress τ_0/τ_{w1}

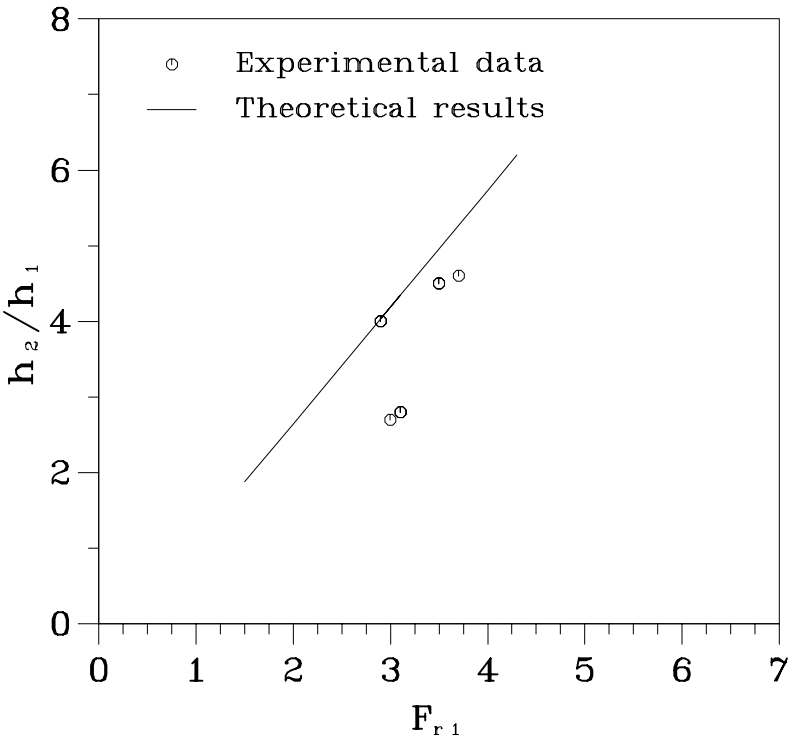

Figure 8: Comparison of the conjugate depth

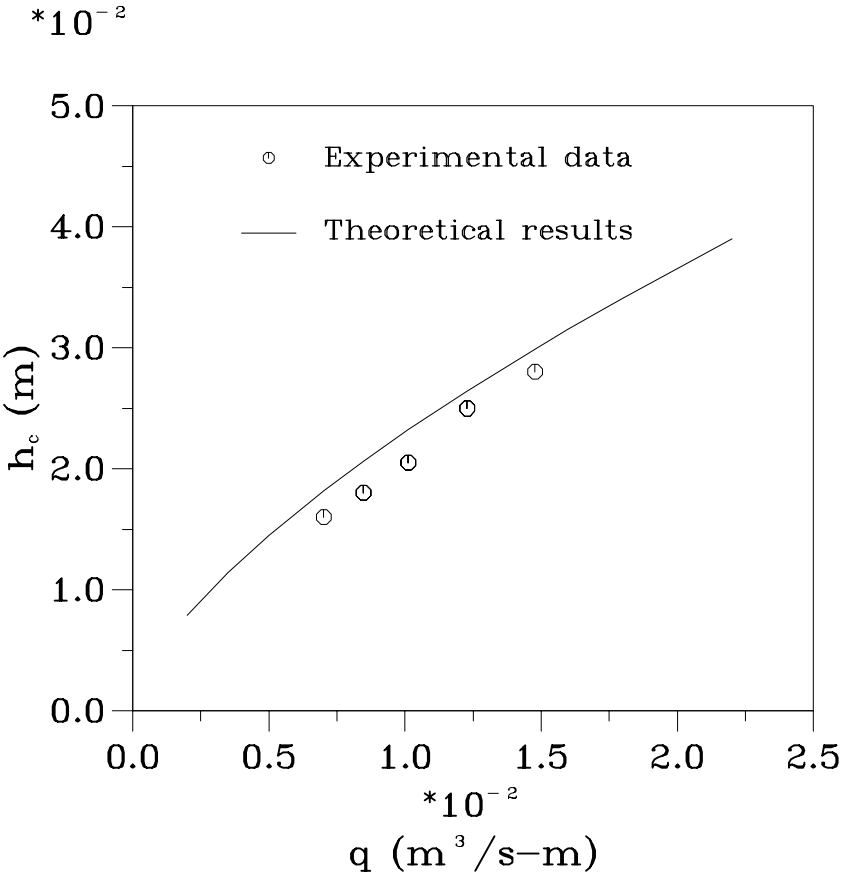

Figure 9: Comparison of the critical depth